ICES Journal of Marine Science
July 2009, Volume 66 (6) : Pages 1410-1416
http://dx.doi.org/10.1093/icesjms/fsp039

The influence of the environment on the variability of monthly tuna biomass around a moored, fish-aggregating device

Mathieu Doray[1, *], Pierre Petitgas[1], Laetitia Nelson[2], Stéphanie Mahévas[1], Erwan Josse[3], and Lionel Reynal[2]

[1] Ifremer, EMH, Rue de l'Ile d'Yeu B.P. 21105 44311, Nantes, Cedex 03, France
[2] Ifremer, Laboratoire Ressources Halieutiques Antilles, Pointe Fort, 97321 Le Robert, Martinique
[3] IRD, US acoustique halieutique, centre IRD de Bretagne, BP 70, 29280 Plouzané France

*: Corresponding author : Mathieu Doray, 332 40 37 41 65; fax: 332 4037 4001; email address : mathieu.doray@gmail.com

Abstract:

Fish-aggregating devices (FADs) are increasingly used worldwide to enhance tuna catches. Meanwhile, ecosystem-based management of this fishery is constrained by a paucity of information regarding the interaction of FAD-associated tuna aggregations with their local environment. This paper reports the results of a nine-month study around a FAD moored near Martinique Island, aimed at assessing the effects of the local environment on the variability of monthly estimates of proximate tuna biomass. Dual-frequency, active acoustics provided highresolution quantitative data on the pelagic community around the FAD, from fish to micronekton forage. Geostatistics were used to compute biomass estimates of the tuna aggregation comprising most of the FADassociated fish biomass, with a sampling error of 27%. Environmental variability was summarized by a small set of principal components (PCs) derived from profiles of temperature, salinity and dissolved oxygen vs. depth; and maps of chlorophyll a derived from remotely sensed, sea-surface colour. A generalized linear model was used to relate tuna biomass to environmental PCs and revealed a positive correlation between tuna abundance and: i) a micronekton layer sensed at 38 kHz and potentially consisting of preferred prey at about 180 m depth; and ii) low subsurface salinity (60–80 m). These favourable environmental conditions may be related to thepresence of North Brazilian Current eddies that migrating tuna follow when not temporally associated with the FADs.

Keywords: fish-aggregating device, biomass estimation, geostatistics, environment, tuna, Lesser Antilles

Introduction

Large pelagic fish (tuna, dolphinfish and billfish) concentrate around fish-aggregating devices (FADs). Consequently, deployments of FADs have facilitated the development of small- and large-scale fisheries worldwide (Fonteneau *et al.*, 2000) and provided opportunities for studying the behaviours of large pelagic fish (Girard *et al.*, 2004; Josse *et al.*, 2000; Moreno *et al.*, 2007). Most of these studies used echosounders to acquire high-resolution quantitative data on the pelagic community near FADs, ranging from fish aggregations to micronekton forage. The studies were done over periods ranging from hours to weeks and were focused on the structure of fish aggregations around moored FADs (Doray *et al.*, 2006; Doray *et al.*, 2007; Josse *et al.*, 2000) and drifting FADs (Moreno *et al.*, 2007). However, unbiased stock-assessment models require a better understanding of the natural, large-scale dynamics of fish biomass aggregated around FADs as related to environmental forcing (Fonteneau *et al.*, 2000). The objective of this study was to model the monthly variations of tuna biomass associated with a moored FAD as a function of the local biotic and abiotic environment.

Methods

Overview

This paper is based on the data and findings of a nine-month study conducted around a FAD moored near Martinique island, Lesser Antilles (Doray *et al.*, 2006; Doray *et al.*, 2007; Doray *et al.*, 2008). Doray *et al.* (2006, 2007) demonstrated that the fish around the FAD were dominated by a single aggregation of tuna made up of mostly blackfin tuna (*Thunnus atlanticus*), some yellowfin tuna (*Thunnus albacares*), and skipjack (*Katsuwonus pelamis*), located at depths ranging from 30 to 100 m.

For this paper, maxima of daily tuna biomass and confidence intervals were computed from the acoustic backscatter recorded around the FAD, using the geostatistical universal kriging method (GUK) designed by Doray *et al.* (2008). The abiotic (hydrography) and biotic (micronekton forage) environment around the FAD during the same period are summarized by a small set of principal components (PCs) derived from a Principal

Component Analysis (PCA). A generalized linear model (GLM) is used to elucidate the relationships between the daily tuna biomass maxima and the environmental PCs.

Data

Acoustic data collection

From August 2003 to April 2004, the French Institute for the Exploitation of the Sea (Ifremer) did nine surveys, one each month, around a FAD moored at depths of 2500 m, at a distance of 25 nautical miles from the leeward coast of Martinique. The FAD was floated with two groups of buoys (heads). Surveys were done from the chartered 12 m fishing vessel, FV "Béryx", which was equipped with 38 and 120 kHz echosounders (Simrad EK60, firmware version 1.4.6.72) connected to two hull-mounted, split-beam transducers (ES38-B and ES120–7G, respectively), each with a 7° beam width (Doray *et al.*, 2006). Pulse lengths were 512 µs for both frequencies. The echosounders were calibrated before each cruise, using a standard sphere (Foote, 1982).

To observe complete diel cycles and estimate inter-day biomass variability, the FAD was surveyed over multiple 72 hour periods (legs). Each leg began around 12:00 on the first day and ended around 14:00 on the third day. In October 2003, and April 2004, the FAD was respectively surveyed for five and two extra days. An average of ten small star acoustic surveys (SSS; Josse *et al.*, 2000) were conducted per daytime period within a radius of 400 m around both heads of the FAD, totalling 214 SSS. Where the starting times, t_1 and t_2, were separated by less than an hour, the results were considered a dual survey (DS). DSs were used to assess the total tuna biomass around both heads of the FAD at time $t_m = (t_1 + t_2)/2$. Complementary large star surveys (LSS) were conducted once around midday and once around midnight within a 1500 m radius of the FAD heads, totalling 47 LSS. SSS and LSS were on average completed within 0.5 and 2 hours, respectively. For further details, see Doray *et al.* (2006, 2007).

The FAD was located more than 10 km from other known moorings. Tuna may detect a moored FAD from a range of 10 km (influence radius; Girard *et al.*, 2004). The tuna biomass around the FAD was thus assumed to be unaffected by the presence of another mooring. The nine-month observation series (August 2003 to April 2004)

is the longest available.

Abiotic environment descriptor

Every 24 hours, profiles of salinity, temperature, and dissolved oxygen vs. depth (pressure) were recorded (SBE 19 CTD; Sea-Bird Electronics, Inc.) to depths of 600 m near the moored FAD (mean number of profiles per leg = 3; s.d. = 1.9). The CTD was lowered and raised at a constant speed of 1 m s^{-1} and all data were averaged within 10 m depth layers.

Biotic environment descriptors

Weekly composite maps of surface chlorophyll *a* (Chl *a*) concentration covering the Lesser Antilles area with a 4 km resolution were used to assess the surface-phytoplankton productivity during the sea cruises. These maps were generated with data from the Sea-viewing Wide Field-of-view Sensor (SeaWiFS; http://eosdata.gsfc.nasa.gov/data/dataset/SEAWIFS/). Chl *a* values collected over two-day periods were averaged over eight-day periods to smooth the data compromised by clouds. These maps were scrutinized for the presence of Amazonian river water (ARW), known to influence the Lesser Antilles area throughout the year (Hu *et al.*, 2004). ARW plumes flow throughout the archipelago, reaching their maximum surface coverage from June to November. From November to February (Hu *et al.*, 2004), some of the plumes moving through the Lesser Antilles are trapped into large anticyclonic eddies shed by a retroflection of the North Brazilian Current (NBC). Mean Chl *a* concentrations computed in the 16 km^2 SeaWiFS grid cell surrounding the FAD during the surveyed month *m* were extracted and denoted as *mChla*(*m*).

The vertical structures and densities of micronekton sound-scattering layers (SSLs) were assessed by the integrated volume-backscattering coefficients ($s_{A;}$ averaged in 15 m^2 cells) collected at both frequencies during 47 LSS (mean number of surveys per leg = 5, s.d. = 3; including 25 daytime and 22 night-time surveys). First, the volume-backscattering strengths were thresholded at –75 dB to exclude noise and scatter from non-micronekton, while retaining scatter from the most relevant micronekton (Bertrand *et al.*, 1999). Then, s_A was calculated from 10 to 600 m and 10 to 200 m at 38 and 120 kHz, respectively. To exclude tuna concentrated near

the FAD from the SSL density estimates, data collected within 350 m of the FAD head were excluded.

Micronekton layers near the FAD were sampled between 0 and 100 m depth with a mesopelagic trawl (4 mm mesh; 7 m² mouth). The average catches of the 46 hauls were dominated in weight by gelatinous organisms (43%), fish (34%), and crustaceans (19%; J. Chantrel, unpublished data). Total counts of non-gelatinous organisms were dominated by crustaceans (69%), fish (23%), and molluscs (7%; Nelson *et al.*, 2007). Crustaceans were mostly stomatopods and euphausiids of mean total length = 25 mm. These organisms have a very low target strength (≈ –90 dB; Foote *et al.*, 1990), so their scatter was likely below the threshold. Fish abundance was dominated by anguilliforms of mean fork length (L_F) = 62 mm and carangids of mean L_F = 20 mm that would be detected at densities of 1 and 0.03 individuals m^{-3}, respectively, at the –75 dB threshold. Corrected for trawl selectivity (May and Blaber, 1989), the anguilliforms and carangids densities ranged from 0.3 to 9, individuals m^{-3}, respectively. Therefore, the acoustically derived densities of anguilliforms were probably underestimated, whereas it was more accurately estimated for fish with swimbladders. However, it is also possible that a significant amount of the 38 kHz backscatter could have resulted from gelatinous micronekton with gas bubbles (Mair *et al.*, 2005).

Characterization of environmental conditions

The abiotic environment was described by 87 variables (j = 1 to 87) derived from the profiles of temperature, salinity, and dissolved oxygen, averaged over 10 m depth layers from 5 to 285 m. Let $X.CTD_j(m,c)$ denote the j^{th} CTD variable recorded during the c^{th} CTD cast during month m.

Diel variations in the vertical structure of the SSLs were appreciable so the daytime and night-time SSL profiles were analysed separately. The vertical structure of the SSL in the LSSs was represented by s_A profiles at 38 and 120 kHz, each with 10 m depth resolution Let $X.SSLDNf_k(m,l)$ denote the SSL acoustic densities recorded during the daytime or night-time diel period DN at frequency f = 38 or 120 kHz in the k^{th} depth layer (k = 1 to 39, and 1 to 19, respectively) surveyed during LSS l and month m. Monthly averages of $mX.CTD_j$ and $mX.SSLDNf_k$ variables, referred to as $mX.CTD_j(m)$ and $mX.SSLDNf_k(m)$, were first computed. Global monthly indices of

temperature, salinity, oxygen, and micronekton densities, denoted $mX.CTD(m)$ and $mX.SSLDNf(m)$, were subsequently calculated by averaging $mX.CTD_j(m)$ and $mX.SSLDNf_k(m)$ over depth.

A matrix **X** was formed by $mX.CTD_j(m)$, $mX.SSLDNf_k(m)$, $mX.CTD(m)$, $mX.SSLDNf(m)$ and $mChla(m)$ to represent the mean environmental conditions around the offshore FAD. **X** was centered-scaled by columnsand input to a PCA to reduce its 193 variables to a more tractable set of variables, while conserving most of the information. The PCA explained 100% of the total variance with eight ordination axes. The orthogonal PCs ($PC_i(m)$; i ranging from 1 to 8), were eventually selected to summarize the biotic and abiotic environmental conditions encountered during m around the FAD.

Tuna biomass estimates

To extract the tuna shoals from the dense surrounding scattering layers (Doray *et al.*, 2006), the 120 kHz echograms recorded during 160 SSS (124 daytime and 36 night-time) were processed with an image-analysis algorithm implemented in Movies+ (Weill *et al.*, 1993). The s_A attributed to tuna were averaged over 15 m track-line lengths. Average tuna s_A per survey was computed, summed by DSs, and averaged by hour, to assess the diel variations of tuna biomass around the FAD. The daily tuna biomass maximum $DS_{max}(d)$, defined by the highest s_A in a 24 h period, was computed for each day d during each dual survey. The $DS_{max}(d)$ represented the maximum daily tuna biomass observed around the FAD from August 2003 to April 2004 (n = 32, mean number of DS per month = 3.6, s.d. = 1.3).

The geostatistical method proposed by Doray *et al.* (2008) was applied to this subset of surveys, to compute estimates of biomass and sampling error for tuna aggregations sampled with a star acoustic survey (see Rivoirard *et al.* (2001) for comprehensive information on the applications of geostatistics for estimating fish abundance). This method aims to: (a) record the position of the head of the FAD during the survey; (b) reference the sample positions relative to the FAD's head; (c) centre the sample positions relative to the tuna aggregation gravity centre and normalize the sample positions using the standard deviation (s.d.) of the positions; (d) grid the tuna aggregation area V, and estimate the average fish density in each cell; (e) normalize each cell value by the survey

average in area *V* and estimate relative densities; (f) do (a) to (e) for each survey of the subset of daily biomass maxima and estimate the average relative density surface across surveys; (g) model the deterministic component in the relative density surface (i.e. model the decrease in average relative density from the centre of the aggregation to its borders, using a one-dimensional advection–diffusion model of animal grouping; Okubo *et al.*, 2001); (h) estimate two-dimensional residuals in each cell for each survey: (i) estimate a variogram for the residuals: and (j) estimate the survey mean and its precision by kriging (see Doray *et al.*, 2008 for details). For simplicity, the survey mean is the arithmetic mean rather than the kriged mean. The tuna aggregation area *V* was defined as the circular area (160 m radius) centred on the aggregation gravity centre. The estimation error is expressed as the geostatistical standard error:

$$SE = \frac{\sigma_E}{E\left[Z_V(t)\right]}, \quad (1)$$

where σ_E is the square root of the geostatistical estimation of variance and; $E[\ ]$ is a time-average operator; and $Z_V(t)$ is the daytime mean acoustic densities of tuna in area *V* and survey *t*. The abundance *A* (number of fish) and biomass *B* (tons) of tuna were computed in *V* for each survey *t* (Doray *et al.*, 2008):

$$A(t) = V\rho_A = V\frac{Z_V(t)}{\langle \sigma_{bs} \rangle} \text{ and } B(t) = A(t)\frac{\overline{W}}{1000}, \quad (2)$$

where ρ_A is the density of tuna within the aggregation of area *V* (fish m^{-2}); $\langle \sigma_{bs} \rangle$ = 3.2 10^{-4} m^2 is the mean backscattering cross section (MacLennan *et al.*, 2002); and $\overline{W}$ = 2.7 kg is the mean weight of a single tuna (the same constants were used in Doray *et al.*, 2008). Confidence intervals $CI_{geo}(t)$ were calculated for each of the maxima of tuna biomass *B* as $CI_{geo}(t) = B(t) \pm (t) \times SE$. Global monthly confidence intervals $CI_{geo\text{-}tot}(m)$ were also computed as the range of the $CI_{geo}(t)$ of month *m*.

Temporal dynamics of tuna biomass and its relation to the environment

Because not all the confidence intervals around successive monthly biomass maxima overlapped, mean tuna

biomass maxima per month m $\overline{B}(m)$ were calculated. The presence of temporal autocorrelation was investigated by fitting an ARIMA model (Harvey, 1993) to the $\overline{B}(m)$ time-series. Monthly averages and variances of tuna biomass maxima were compared, to assess the effect of monthly abundance fluctuations on the inter-day variability of tuna abundance.

Daily tuna biomass maxima were then modelled as a function of monthly environmental PCs, using GLMs with a gamma error distribution. The simplest model was selected by dropping terms until the Akaike Information Criterion (AIC; Sakamoto *et al.*, 1986) was minimized and residuals were normal. This best model was used to compute GLM estimates of monthly tuna biomass $\hat{B}$ and confidence intervals CI_{GLM}. However, the use of PCs to describe environmental conditions makes the ecological interpretation of GLM results less transparent. Consequently, correlations were calculated between tuna biomass maxima, *B,* and a matrix **X.PCs** comprising the PCs variables that were significant in the best GLM. *B* is an illustrative variable in the ordination space defined by **X.PCs.** Also illustrative, are the mean environmental conditions encountered during each leg and groups of **X** variables contributing most to the ordination along **X.PCs** axes. These groups were defined by selecting the **X** variables whose norms in the **X.PCs** space were higher than those of a variable contributing equally to the eight ordination axes (i.e. higher than 3/8 = 0.375 in a three-dimensional space; see Legendre and Legendre 1998). Similar monthly environmental conditions were clustered using Hierarchical Agglomerative Clustering (HAC ;Hartigan, 1975) on **XP.PCs**. To assess consistency of the model results to the geostatistical estimation errors, the mean monthly biomass and 95% confidence intervals (CI_{GLM}) derived from the best GLM were plotted over confidence intervals calculated for each monthly cruise $CI_{geo\text{-}tot}$.

Statistics were implemented using the R statistical environment (R Development Core Team, 2007), supplemented with the 'vegan' (Oksanen *et al.*, 2007) and 'MASS' (Venables and Ripley, 2002) packages. Geostatistical computations were implemented using EVA2 software (Petitgas and Lafont, 1997) and R package 'geoR' (Ribeiro and Diggle, 2001).

Results

Tuna biomass estimates

Daily tuna biomass maxima were observed on average at 11:18 (s.d. = 03:13). The average relative density surface across surveys was reasonably isotropic. The fit of the advection–diffusion model of animal groupings within the one-dimensional distribution of tuna kernel density estimates was good (r^2 = 99 %). On average, the two-dimensional residuals of the universal model exhibited moderate spatial autocorrelation. The mean experimental variogram of residuals was modelled using a spherical model γ with a nugget of 4.7, a range of 76 m and the sill at 2.4. Checking procedures (Doray *et al.*, 2008) confirmed that the model reasonably represented the survey data. The global standard error for the star surveys conducted during the daily peaks of tuna biomass was 27%. The maximum mean daily tuna biomass estimated around the FAD during the study period was 7 tonnes (s.d. = 5.4, range 1–24 t), mean estimation error = ±1.9 t.

Temporal dynamics of tuna biomass and relation to environment

Tuna biomass maxima and their confidence intervals (CIs) are represented as a function of time in Figure 1. Non-overlapping CIs indicate two levels of tuna biomass: 1) low levels in September, October, and December 2003, and February and April 2004; and 2) high levels in August and November 2003 and January and March 2004. ARIMA models indicated the absence of significant temporal autocorrelation in the time-series of monthly mean tuna biomass. A significant (r^2 = 0.88), almost identical, linear relationship (slope = 0.9) was found between intra-month variances and intra-month means of tuna abundance, for low to medium mean biomass levels (i.e. excluding observations in January and March 2004; Figure 2).

The best model relating tuna biomass maxima B_i to synthetic environmental PCs was:

$$\frac{1}{E[Bi]} = 0.03PC_2 - 0.01PC_3 + 0.03PC_5 + 0.03PC_6 + 0.02PC_7 + 0.19 + \varepsilon_i \,, \quad (3)$$

where $\varepsilon_i \approx$ gamma, and explains 66% of the biomass variability. GLM predictions and confidence intervals

overlaid on the geostatistical CIs of monthly tuna biomass estimates (Figure 1) revealed good agreement between observed and modelled values, except for very low daily tuna biomass maxima.

An analysis of deviance revealed that PC_2, PC_5 and PC_7 explain significant amounts of tuna biomass variability (19%, 32%, and 12%, respectively) after inclusion of other terms in the model. The projection of tuna biomass maxima is illustrated in the three-dimensional ordination formed by PC_2, PC_5 and PC_7 (Figure 3).

Three clusters of distinct environmental conditions were identified by HAC (Figure 3). Cluster 1 was located to the right in the ordination space (positive PC_2 values). It included data from legs done during the warm season, in August, September, and October 2003, with low salinity near the surface (0–25 m) and mixed warm water, and exhibiting strong 38 kHz SSLs (0–100 m), both during daytime and night-time (Figure 3.1). The December 2003 leg was also included in cluster 1, but was associated with average environmental conditions. Low surface-salinity values observed in cluster 1 is explained by the coincidence of the Orinoco plume in the Chl *a* maps (Figure 3a). Other legs were located to the left in the ordination plane (negative PC_2 values), suggesting a marked change in the FAD environment in early 2004.

Cluster 2 included data from the legs in January and March 2003. It was characterized by negative PC_5 values, representing high 38 kHz SSL densities around 180 m depth and low subsurface salinity (60–80 m). During this period, water around the FAD was relatively cold (below average), well stratified, and characterized by a staircase salinity profile (0–80 m; Figure 3.2). Relative to other clusters, the SSL were homogeneously distributed over a wider vertical range.

Cluster 3 included data from the legs in November 2003, and February to April 2004. It is characterized by environmental conditions resembling those of cluster 2, but with a weaker vertical stratification and higher subsurface salinity. The vector representing tuna biomass in this three-dimensional landscape of influential environmental conditions points towards cluster 2 (Figure 3). High tuna abundance levels recorded in January and March 2003 can thus be related to the presence of dense SSL at about 180 m depth, and to low subsurface salinity.

Maps of Chl *a* indicate the presence of a large eddy immediately after the March 2003 leg (Figure 3b), which later collided with the Lesser Antilles. This might have been an NBC eddy, because the temperature-salinity profiles near the FAD in March 2003 were very similar to those recorded near NBC eddies by Hu *et al.* (2004).

Discussion

This study was the first long-term (nine months) analysis of the temporal dynamics of tuna biomass around a FAD in relation to its local biotic and abiotic environment. Active acoustics played a pivotal role in this work, by providing non-intrusive sampling of both tuna aggregations and micronekton SSLs on multiple temporal scales. Despite the very small spatial scale of this study, the frequent legs spanning a large period provided new insight into the ecological processes.

The relative isotropy of the mean tuna density surface during daily peaks of biomass allowed for a reasonable fit of the universal kriging model. However, the residual spatial correlation was relatively low, with a nugget equal to 66% of the sum of sills in the mean residual variogram model, indicating proximity to the limits of applicability of the advection–diffusion drift model. Nonetheless, the presence of a consistent drift in the tuna spatial distribution during nine months corroborates the hypothesis of Doray *et al.* (2008) that the spatial distribution of tuna aggregations observed at the macroscopic scale may result from identical, time invariant, social behaviour of individual tuna.

Environmental descriptors explained 66% of the tuna biomass variability in the best GLM model. Some of the residual variance may have been caused by density-dependent processes triggering the daily tuna aggregation cycle around the FAD. Small-scale, social-aggregative processes should modulate the intra-month variability. Indeed, for low-to-average tuna abundance levels, tuna biomass variability increased with monthly mean tuna abundance. This result may indicate that the residence time of fish around the FAD increased when the global abundance was low. Conversely, the increase of monthly mean global tuna biomass and variance observed around the FAD may be caused by the presence of a larger number of mobile tuna, with lower residence times (i.e. less than three days), undergoing migrations at meso- or regional scales. The fact that intra-month means

and variances of tuna abundance are roughly equal, also suggests that daily abundance maxima may follow a Poisson distribution, thus implying random temporal distribution. In this case, the maximum level of biomass observed around the FAD on a given day would be independent of the biomass levels observed on previous days around the same FAD.

PCA allowed the complex FAD environment to be represented by a small set of uncorrelated PCs, while preserving most of the original variance. The small number of orthogonal PCs summarizing the environment facilitated the fit of regression models with fewer degrees of freedom (n = 32). Regression results were represented by projecting original environmental variables and tuna biomass in the ordination plane that explained a significant part of the tuna biomass variability. This method efficiently identified combinations of depth strata and environmental descriptors that explained much of the variability in tuna biomass.

Which ecological processes explain the statistical correlations between tuna biomass and environmental descriptors? Tuna aggregations were always located in the preferred mixed layer (Bertrand *et al.*, 2002; Sund *et al.*, 1981). Thus, the significant abiotic environmental descriptors were not directly forcing the FAD tuna biomass, but might have been indicative of seasonal tuna migratory patterns. Indeed, trends in the catches of artisanal, moored FAD fisheries in Martinique (Doray *et al.*, 2002) and Guadeloupe (Diaz *et al.*, 2002) suggest that large yellowfin leave the Southern Lesser Antilles area to migrate North during the first and fourth quarters. High tuna biomass levels observed around the offshore FAD during the first quarter of 2004 might have been because of transient yellowfin tuna. Moreover, such tuna migrations may be triggered or related to seasonal fluctuations of the regional oceanography. The negative correlation between tuna biomass and subsurface salinity, and the presence of a NBC eddy near Martinique during the March 2004 tuna biomass peak, suggest that tuna may follow the low subsurface salinity in NBC eddies. Tuna may favour these areas to feed on micronekton prey sustained by the higher surface primary production observed at the periphery of the eddies. Trophic interaction between tuna and SSLs as observed around the FAD, is corroborated by the positive correlation between FAD tuna biomass and the daytime SSL at 180 m, which might have consisted of preferred prey.

SSL densities proved to be a better proxy of the prey availability around the FAD than the Chl *a* values, which were not strongly correlated with tuna biomass. However, the micronekton prey density in this study poorly accounted for the crustacean component of the prey assemblage, which may represent a substantial part of the diets of tuna associated with FADs (Grubbs *et al.*, 2007). Moreover, the strong acoustic backscatter from gas-bearing gelatinous organisms at 38 kHz might have masked the contribution of other SSL components to the total backscatter (Mair *et al.*, 2005). The negative correlation between 38 kHz SSLs with gelatinous organisms and tuna during the warm season may not indicate a shortage of tuna prey, but rather support conventional thinking that tuna do not eat jellyfish.

This study did not span a complete annual cycle, so the identified forcing exerted by regional oceanography on FAD-associated tuna may not be valid on broader scales. However, the results do suggest a correlation between FAD-related tuna abundance and fish abundance at larger scales, perhaps justifying the use of local tuna abundances to estimate mesoscale tuna indices. Thus, a network of FADs instrumented with autonomous echosounders and environmental sensors may be useful for direct, near real-time monitoring of tropical pelagic ecosystems.

Acknowledgments

This research was co-funded by the European Community, and the Regional Council and Prefecture of Martinique. The authors are grateful to the crew of the FV “Béryx” for their invaluable assistance during the sea cruises. We are also grateful to D. Dagorne (Insitut de Recherché pour le Développement, US Imago) for providing Chl *a* maps. The referees and the guest editor are thanked for thoughtful comments, which greatly improved the manuscript.

References

Bertrand, A., Josse, E., Bach, P., Gros, P., and Dagorn, L. 2002. Hydrological and trophic characteristics of tuna habitat: consequences on tuna distribution and longline catchability. Canadian Journal of Fisheries and Aquatic Sciences, 59: 1002–1013.

Bertrand, A., Le Borgne, R., and Josse, E. 1999. Acoustic characterisation of micronekton distribution in French Polynesia. Marine Ecology Progress Series, 191: 127–140.

Diaz, N., Doray, M., Reynal, L., Gervain, P., and Carpentier, A. 2002. Pêche des poissons pélagiques hauturiers et développement des DCP ancrés en Guadeloupe. FAO Fisheries Report, 683, Supplement: 39–54.

Doray, M., Josse, E., Gervain, P., Reynal, L., and Chantrel, J. 2006. Acoustic characterisation of pelagic fish aggregations around moored fish aggregating devices in Martinique (Lesser Antilles). Fisheries Research, 82: 162–175.

Doray, M., Josse, E., Gervain, P., Reynal, L., and Chantrel, J. 2007. Joint use of echosounding, fishing and video techniques to assess the structure of fish aggregations around moored Fish Aggregating Devices in Martinique (Lesser Antilles). Aquatic Living Resources, 20: 357–366.

Doray, M., Petitgas, P., and Josse, E. 2008. A geostatistical method for assessing biomass of tuna aggregations around moored Fish Aggregating Devices with star acoustic surveys. Canadian Journal of Fisheries and Aquatic Sciences, 65: 1193–1205.

Doray, M., Reynal L., Carpentier, A., and Lagin, A. 2002. Le développement de la pêche associée aux DCP ancrés en Martinique. FAO Fisheries Report 683, Supplement: 69–88.

Fonteneau A., Pallarés, P., and Pianet, R. 2000. A worldwide review of purse seine fisheries on FADs. In Le Gall, J. Y., Cayré, P., Taquet, M., Cayré, P., and Taquet, M. (Eds.). *Tuna Fishing and Fish Aggregating Devices Symposium*. Actes Colloq, Ed. Ifremer, 28: 15–35.

Foote, K., Everson, I., Watkins, J. L., and Bone, D. G. 1990. Target strengths of Antarctic krill (*Euphausia superba*) at 38 and 120 kHz. Journal of the Acoustical Society of America, 87: 16–24.

Foote, K. G. 1982. Optimizing copper spheres for precision calibration of hydroacoustic equipment. Journal of the

Acoustical Society of America, 71: 742–747.

Girard, C., Benhamou, S., and Dagorn, L. 2004. FAD: Fish Aggregating Device or Fish Attracting Device? A new analysis of yellowfin tuna movements around floating objects. Animal Behaviour, 67: 319–326.

Grubbs, D., Holland, K., and Itano, D. 2007. Comparative trophic ecology of yellowfin and bigeye tuna associated with natural and man-made aggregation sites in Hawaiian waters. SCTB15 Working Paper, YFT-6: 1–20.

Hartigan J.A., 1975. Clustering Algorithms. Wiley, New York, USA, xiii+351 pp.

Harvey, A. C. 1993. Time Series Models, Second Edition, Harvester Wheatsheaf, London.

Hu, C., Montgomery, E. T., Schmitt, R. W., and Muller-Karger, F. E. 2004. The dispersal of the Amazon and Orinoco river water in the Tropical Atlantic and Caribbean Sea: Observation from space and S-PALACE floats. Deep Sea Research, 51: 10–11.

Josse, E., Dagorn, L., and Bertrand, A. 2000. Typology and behaviour of tuna aggregations around fish aggregating devices from acoustic surveys in French Polynesia. Aquatic Living Resources, 13: 183–192.

Legendre, P., and Legendre, L. 1998. Numerical Ecology. Elsevier, Amsterdam.

MacLennan, D. N., Fernandes, P. G., and Dalen, J. 2002. A consistent approach to definitions and symbols in fisheries acoustics. ICES Journal of Marine Science, 59: 365–369.

Mair, A., Fernandes, P., Lebourges-Dhaussy, A., and Brierley, A. 2005. An investigation into the zooplankton composition of a prominent 38-kHz scattering layer in the North Sea. Journal of Plankton Research, 27: 623–633.

May, J. L., and Blaber, S. J. M. 1989. Benthic and pelagic fish biomass of the upper continental slope off eastern Tasmania. Marine Biology, 101: 11–25.

Moreno, G., Josse, E., Brehmer, P., and Nøttestad, L. 2007. Echotrace classification and spatial distribution of pelagic fish aggregations around drifting fish aggregating devices (DFAD). Aquatic Living Resources, 20: 343–356.

Nelson L., Reynal L. and Chantrel J., 2007. Density and biomass variations of micronekton close to fish aggregating devices (FADs) around Martinique. Gulf and Caribbean Fisheries Institute Proceedings, 59: 549-556.

Oksanen, J., Kindt, R., Legendre, P., O'Hara, B., and Stevens M. 2007. vegan: Community Ecology Package. R package,

version 1.8–8: http://cran.r-project.org/, http://r-forge.r-project.org/projects/vegan/

Okubo, A., Grünbaum, D., and Edelstein-Keshet, L. 2001. The Dynamics of Animal Grouping. In Okubo, A. and Levin, S. A. (Eds.). Diffusion and ecological problems: Modern Perspectives. Second Edition. Springer-Verlag, Berlin, 197–237.

Petitgas, P., and Lafont, T. 1997. EVA2: Estimation variance. Version 2. A geostatistical software on Windows 95 for the precision of fish stock assessment surveys. ICES Document CM, 1997/Y:22.

R Development Core Team, 2007. R: A language and environment for statistical computing. R Foundation for Statistical Computing, Vienna, Austria. ISBN 3–900051–07–0, URL http://www.R-project.org.

Ribeiro, P., and Diggle, P. 2001. geoR: a package for geostatistical analysis. R-NEWS, 1: 15–18.

Rivoirard, J., Bez, N., Fernandes, P., Foote, K., and Simmonds, J. 2000. Geostatistics for Estimating Fish Abundance. Blackwell Science, Oxford.

Sakamoto Y., Ishiguro M. and G K., 1986. Akaike Information Criterion Statistics. D. Reidel Publishing Company, Dordrecht, Holland, 320 pp.

Sund P., Blackburn M., and Williams, F. 1981. Tunas and their environment in the Pacific Ocean: A review. Oceanography and Marine Biology Annual Review. 19: 443–512.

Venables, W., and Ripley, B. 2002. Modern Applied Statistics with S. Fourth Edition. Springer, New York.

Weill, A., Scalabrin, C., and Diner, N. 1993. MOVIES-B: An acoustic detection description software. Application to shoal species' classification. Aquatic Living Resources, 6: 255–267.

Figure captions

Figure 1. Time-series of daily tuna biomass maxima (black dots) and their confidence intervals (whiskers) estimated around the offshore Fish-Aggregating Device, with generalized linear-model estimates of monthly averages of tuna biomass (bold straight line) and their confidence intervals (grey area) overlaid.

Figure 2. Intra-month variances of tuna biomass maxima, *varB*, as a function of intra-month means of tuna biomass maxima *mB*. Straight line: linear model of the form: $varB = 0.9 \times mB$ ($R^2 = 0.88$), fitted for all months except January and March 2004.

Figure 3. Ordination biplot illustrating the correlations between tuna biomass (broken red arrow) and significant descriptors of environmental conditions encountered around the offshore fish-aggregating device during nine legs conducted from August 2003 to April 2004. Arrows indicate environmental variables contributing more than average to the ordination space. Positions of legs in the ordination plan are indicated using a 'month-year' label and their associations to HAC clusters using different point types. Insets 1 to 3 represent the vertical profiles of mean environmental conditions encountered in HAC clusters 1 to 3: temperature in red; salinity in blue; mean log-transformed daytime (lsA38D) and night-time (lsA38N) 38 kHz acoustic densities of sound-scattering layers in green and pink, respectively. Inset a and b represent SeaWiFS weekly composite Chl *a* map of the Lesser Antilles area corresponding to the October 2003 (a) and March 2004 (b) legs, respectively. The Orinoco plume and a North Brazilian Current eddy are visible on insets a and b, respectively. The study area is located by a bold rectangle.

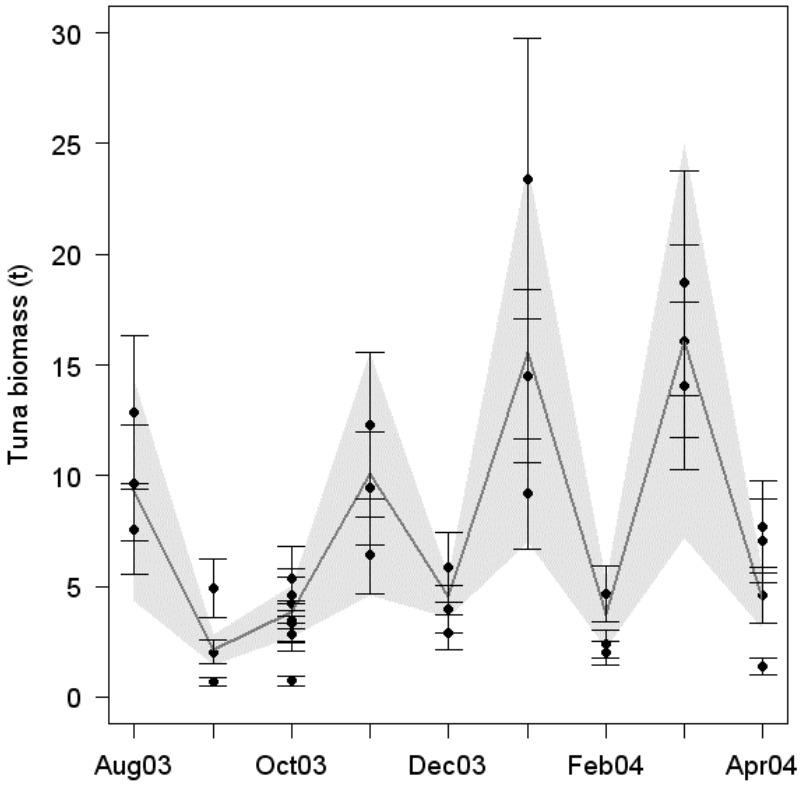

Figure 1.

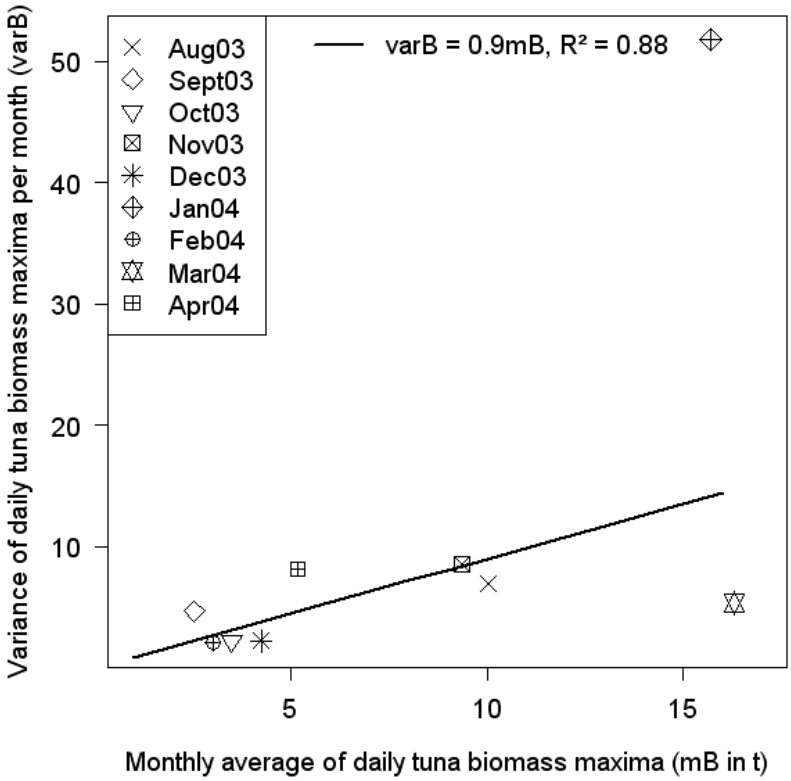
Variance of daily tuna biomass maxima per month (varB)
Monthly average of daily tuna biomass maxima (mB in t)
varB = 0.9mB, R² = 0.88
Aug03
Sept03
Oct03
Nov03
Dec03
Jan04
Feb04
Mar04
Apr04
10
20
30
40
50
5
10
15

Figure 2.

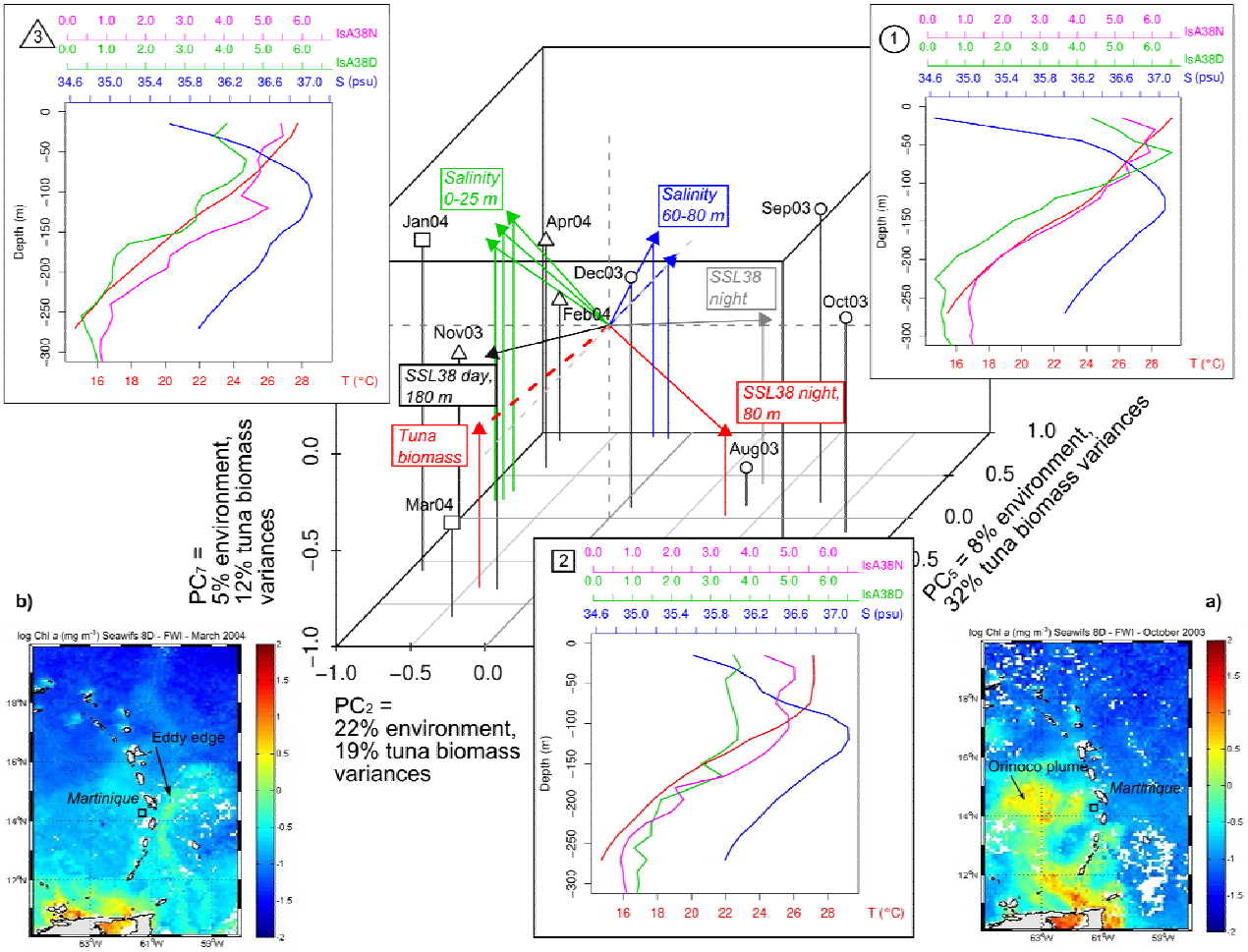
3
1
2
IsA38N
IsA38D
S (psu)
T (°C)
Depth (m)
Salinity 0-25 m
Salinity 60-80 m
SSL38 night
SSL38 day, 180 m
SSL38 night, 80 m
Tuna biomass
Jan04
Feb04
Mar04
Apr04
Dec03
Nov03
Oct03
Sep03
Aug03
PC7 = 5% environment, 12% tuna biomass variances
PC2 = 22% environment, 19% tuna biomass variances
PC5 = 8% environment, 32% tuna biomass variances
b)
a)
Eddy edge
Martinique
Orinoco plume

Figure 3.